

# Sustainable production of silver nanoparticles from waste part of *Litchi chinensis* Sonn. and their antibacterial evaluation

**Amina Hussain**

Department of Environmental Sciences, Fatima Jinnah Woman University, Rawalpindi, Pakistan

**Abstract:** In our study, waste parts of *Litchi chinensis* cultivar Surakhi were selected for the production of silver nanoparticles. Qualitative and quantitative analysis revealed peel extracts rich in alkaloids, flavonoids, saponins, steroids, phenolics, tannins as compared to seed extracts. Two different types of nanoparticles (PAN and PMN) were prepared from *Litchi chinensis* peel using crude aqueous and methanolic extracts. During synthesis, colour variations were observed (brown to blackish brown) and were characterized by UV VIS spectrophotometry. Protein and alkaloids as powerful stabilising agents forming silver nanoparticles were verified by FTIR. Scanning electron microscopy (SEM) analysis of silver nanoparticles shown to be less homogeneous and spherical in form. For PAN and PMN the particle size of silver nanoparticles was 6.9 nm and 7.9 nm respectively with the primitive face-centered cubic phase measured from the XRD pattern. Energy dispersive X-ray spectrometers profile confirmed the strong signal for elemental silver. The antibacterial activity of PAN and PMN against a diverse group of gram positive and gram negative bacterial strains were determined using an agar well diffusion assay. Both types of silver nanoparticles prepared were found effective against *Alcaligenes faecium* with highest antibacterial activities recorded (20mm±0.14 and 18mm±0.14). Minimal inhibitory concentration was found to be 15µg/ml for both PAN and PMN against *Alcaligenes faecium*.

**Keywords:** Green synthesis, quantitative analysis, silver nanoparticles, *Litchi chinensis*, antibacterial activity, fruit peel.

## INTRODUCTION

Nanotechnology solicitation is imperative day by day and nanoparticles of several kinds are manufactured and attaining additional consideration due to their appealing possessions. Even though physical and chemical approaches are prevalent for amalgamation of nanoparticle, the usage of lethal composites diminishes their uses. In order to overcome this difficulty, nontoxic sustainable green approaches consume a vigorous part in producing nanoparticles. Applications of silver nanoparticles comprises optical, textile, engineering, electronics and furthermost prominently in the medical field as a bactericidal and as a therapeutic agent. The high reactivity of silver nanoparticles plays a role in inhibiting microbial activity because of the large surface to volume ratio (Chenthamara *et al.*, 2019).

In this research, we developed less expensive, flexible and highly reproducible procedure for the synthesis of AgNPs utilizing fruit extracts through a reduction reaction. *Litchi chinensis* Sonn. a species of the Surakhi family cultivar of the Sapindaceae family, mainly grown in Pakistan, is considered an interest in a nanoparticles development study that acts both as a reduction and stabilizing agent. *Litchi chinensis* is a tropical fruit that is grown in China and other countries around the globe because of its appealing taste. *Litchi chinensis* is a Chinese tropical grown fruit and its name comes from Lizhi which is a Chinese word, means leaving branches. It is preferred due to its nutritive value (Vitamin C, A, B, calcium) and

\*Corresponding author: e-mail: amina.hussain878@gmail.com

sweet taste. *Litchi chinensis* shows therapeutic values and are effective in glands enlargement, tumors and gastralgia (Emanuele *et al.*, 2017). Antimicrobial and antioxidant, anticancer properties of *Litchi chinensis* has been studied (Zhao *et al.*, 2020). *Litchi chinensis* bark, roots and flowers are used in throat ailments. Roots of *Litchi chinensis* trees have shown activity against tumors in animal models (Khan *et al.*, 2020). It shows varied medicinal effects comprising antibacterial, anti-hyperglycemic, anti-genotoxic, anti-hyperlipidemic, antioxidant, anti-diabetic hepatoprotective and anti-tumor activity (Salehi *et al.*, 2019; Kifle *et al.*, 2020).

The current research focuses to evaluate bio reduction of *Litchi chinensis* fruit extracts from silver ions present in the silver nitrate solution. Waste part of fruit such as peel and seeds were selected in this study. Nanoparticle synthesis was identified and characterized by using different techniques. In addition, multiple multi drug resistant pathogens were evaluated against these biologically produced nanoparticles.

## MATERIALS AND METHODS

### *Preparation of extracts*

*Litchi chinensis* fruit cultivar Surakhi was collected from Khan Pur Orchards, Pakistan. *Litchi chinensis* samples were placed in sterilized bags and transported to laboratory for further analysis. *Litchi chinensis* fruit were authenticated at Department of Botany, Quaid-e-Azam University, Pakistan. Fruits were washed, dried, peeled

and shade dried up to 20 days until dried and grinded into fine powder. For the preparation of extracts according to the methods stated by (Pirtarighat *et al.*, 2019) with some modifications. Two solvents presenting different polarities, i.e. water and methanol, were used.

#### **Phytoconstituent analysis**

Different tests were carried out for screening aqueous and methanolic extracts of *Litchi chinensis* peel and seed. Qualitative phytochemical analysis was performed by Dragendroff's reagent (Potassium bismuth iodide solution) test, Alkaline reagent test, Ferric chloride test, Foam test, Dinitrophenyl hydrazine (DNPH) test with certain modifications to the detection of effective phytochemicals (Mukundi, 2015; Njagi E N Mwaniki *et al.*, 2015; Iqbal *et al.*, 2015; Ayoola *et al.*, 2008). Quantitative analysis of *Litchi chinensis* fruit extracts were carried out according to standard procedure of Folin-Ciocalteu method used for the determination of the total phenol, total alkaloids were determined by using Harborne (1973), Bohm and Kocipai-Abyazan (1994) method for Flavanoid, Obadoni and Ochuko for saponins and tannins were determined by AOAC, 2002 method with some modifications.

#### **Biosynthesis of silver nanoparticles**

Double distilled water (100 ml) was taken in the flask and add 0.50gm crude extract of *Litchi chinensis* peel and start stirring for one hour. Silver nitrate (0.1mM) solution and crude extract was prepared in 100ml of distilled water. Two solutions prepared were added, mixed and fixation of various factors was investigated.

#### **Fixation of factors**

Different parameters such as incubation time (1, 3, 6, 12, 24, 48 and 72 hours), different temperatures (25, 35, 45 and 55°C), pH (4, 7 and 8) and various silver nitrate concentrations (0.1, 0.5, 1 and 2mM) were selected to optimize silver nanoparticles production.

#### **Characterization of nanoparticles**

Mixture were examined with UV VIS spectrophotometry (Shimadzu U.V 1602), Fourier Transform Infrared Spectroscopy (Shimadzu FTIR 8400), X-Ray diffractometer (X-ert Pro Banylitical) and Scanning electron microscopy (Oxford Ins (Inca-200) machine coupled to X-ray spectroscopy (EDX).

#### **Antibacterial action of silver nanoparticles**

Agar well diffusion technique was used to conduct antibacterial action of AgNPs against selected pathogenic bacteria (Rautela *et al.*, 2019). Fig. 1 demonstrates the testing of different bacterial strains against crude extract and silver nanoparticles. Various parameters were tested for different samples and their inhibition zone was analyzed after 24-48 h of incubation

#### **Minimum inhibitory concentration (M.I.C)**

With some modifications, minimal inhibitory concentration (MIC) of biosynthesized silver nanoparticles was determined (Rose *et al.*, 2019; Mogana *et al.*, 2020). Bacterial cultures were grown and six test tubes were obtained from each bacterial culture and nutrient broth (2ml) was initially applied and then cultures was added to each test tubes. Various concentration of AgNPs (1µg/ml, 5µg/ml, 10µg/ml, 15µg/ml, 20µg/ml and 25ug/ml) were applied to test tubes and were incubated for one day. After 24 hours of incubation, the MIC was analyzed using spectrophotometers at 600 nm.

#### **STATISTICAL ANALYSIS**

Antimicrobial assays were done in triplicates, and the results were presented as means with standard deviations. The assays were statistically evaluated using two-way analysis of variance (ANOVA). P values less than 0.05 were given statistical significance.

#### **RESULTS**

Phytochemical screening of different chemical compounds (alkaloids, tannin, saponins, flavonoids, and ascorbic acid) were tested in different extracts. Sections of Surakhi peel (aqueous extracts) have positive phenolic, flavonoid, tannin and alkaloid effects. Ascorbic acid present in seeds (aqueous extracts) while no other compounds were detected. Good results for alkaloids, tannins and saponins were shown by Surakhi peel (methanolic extracts). Phenolic, saponins and tannins were weakly present in seeds (methanolic extracts). Qualitative and quantitative study of aqueous and methanolic *Litchi chinensis* peel and seed extracts shown in table 1.

The quantitative study of *Litchi chinensis* reveals that alkaloid content in peel (methanolic) (315+21.89 mg/mg) was found an increased as compared to aqueous counterparts (275+30.21mg/mg). Seed extracts (aqueous and methanolic) did not contain any alkaloid content. More flavonoid content was contained in peel (aqueous) (185+16.11 mg/mg) was found more as compared to peel (methanol) (133+2.21mg/mg). In different extracts of *Litchi chinensis* parts higher amount of saponin contents were present in peel (methanolic) (30+0.2mg/mg) as compare to seed (methanolic) (19.13+3.45mg/mg) and peel (aqueous) (16+2.22 mg/mg). Higher phenolic content can be shown as peel (aqueous) (0.107+0.34mg/mg) followed by peel (methanolic) (0.087+7.16mg/mg) and seed (methanolic) (0.040+14.22mg/mg). Amount of Tannins discovered higher in peel (aqueous) (0.098 ±21.2mg/mg) as compared to peel (methanolic) (0.096 +13.46mg/mg) and seed (methanolic) (0.015±20.10 mg/mg).

**Table 1:** Qualitative (a) and quantitative (b) estimation of different phytoconstituents in peel and seeds of lychee extracts

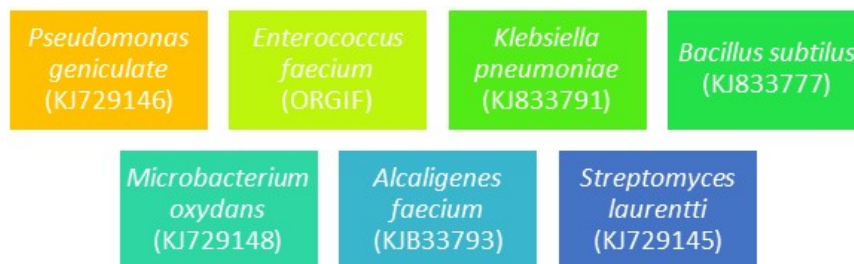
(a)	Aqueous		Methanolic	
	Peel	Seed	Peel	Seed
Compounds				
Phenolic	+++	-	++	+
Flavonoids	+++	-	++	-
Alkaloids	+++	-	+++	-
Tannins	+++	-	+++	+
Saponins	+	-	++	+
Ascorbic acid	-	+++	-	-
(b)	Aqueous		Methanolic	
Compounds	Peel	Seed	Peel	Seed
Phenolic (mg/g)	0.107±0.34	-	0.087±7.16	0.040±14.2
Flavonoids (mg/g)	185±16.11	-	133±2.21	-
Alkaloids (mg/g)	275±30.21	-	315±21.89	-
Tannins (mg/g)	0.098±21.0	-	0.096±13.46	0.015±20.10
Saponins (mg/g)	16±2.26	-	30±0.2	19.13±3.45

Data denotes average of triplicates performed independently, +++ Strongly present, ++ medium present, + weak presence, - absence of compound

**Table 2:** Antibacterial activities of prepared PAN and PMN

Bacterial strains	Control (1mg) (mm)	Plant extract (10mg/ml) (mm)	Silver nitrate (2mg/ml) (mm)	PAN		PMN	
				25µg/ml (mm)	50µg/ml (mm)	25µg/ml (mm)	50µg/ml (mm)
<i>Bacillus subtilus</i>	7.4±0.056	-	6.0±0.05	12±0.1	*15±0.10	15±0.095	*17±0.21
<i>Enterococcus faecium</i>	28±0.10	-	5.0±0.060	8.00±0.04	*10±0.073	10.0±0.05	*12.6±0.30
<i>Klebsiella pneumoniae</i>	20±0.10	-	-	10±0.115	*13±0.10	9.00±0.152	*10±0.10
<i>Streptomyces laurentii</i>	8.0±0.005	-	6.0±0.05	12±0.057	*13±0.060	11±0.057	*12±0.1
<i>Mycobacterium oxidans</i>	32±0.05	-	8.00±0.15	13±0.10	*16±0.20	15±0.064	*17±0.05
<i>Alcaligenes faecium</i>	27±0.10	-	7.00±0.15	15±0.005	*20±0.14	15±0.153	*18±0.1
<i>Pseudomonas geniculata</i>	3.0±0.020	1.0±0.10	10±0.01	10.00±0.03	*13.0±0.10	12±0.10	*15±0.05

-Inhibition zones isn't present, Cefotaxime-USP solution is used as positive control, Data denotes average of triplicates performed independently. \*Asterisk represents a significant difference between PAN and PMN samples different concentrations when two way ANOVA applied.

**Fig. 1:** List of diverse bacterial strain tested against silver nanoparticles

### Visual identification and Fixation of different parameters

PAN extracts revealed a color transition from light brown to a darker color change at ambient temperature after 45 minutes. PMN begins to change color after 15 minutes at 55°C temperature. With increased incubation time, nanoparticles color grew darker brown, and eventually, its color appeared blackish brown.

During the first 45 minutes, the rate of silver ion reduction was slow, as stated by the low absorption value and color change. The optimum condition involved in the

formation of silver nanoparticles, showing a wider peak at 445 nm at ambient temperature after 48 hrs shown in fig. 2. At ambient temperature, PMN did not demonstrate any surface plasmon resonance as shown in fig. 3.

The impact of temperature indicates that after 48 hours, PAN was produced at room temperature. When the temperature was elevated to 35°C and 45°C, the peak width changed to 450nm. Silver nanoparticles shown in fig. 2 did not favour higher temperatures such as 55°C and 65°C.

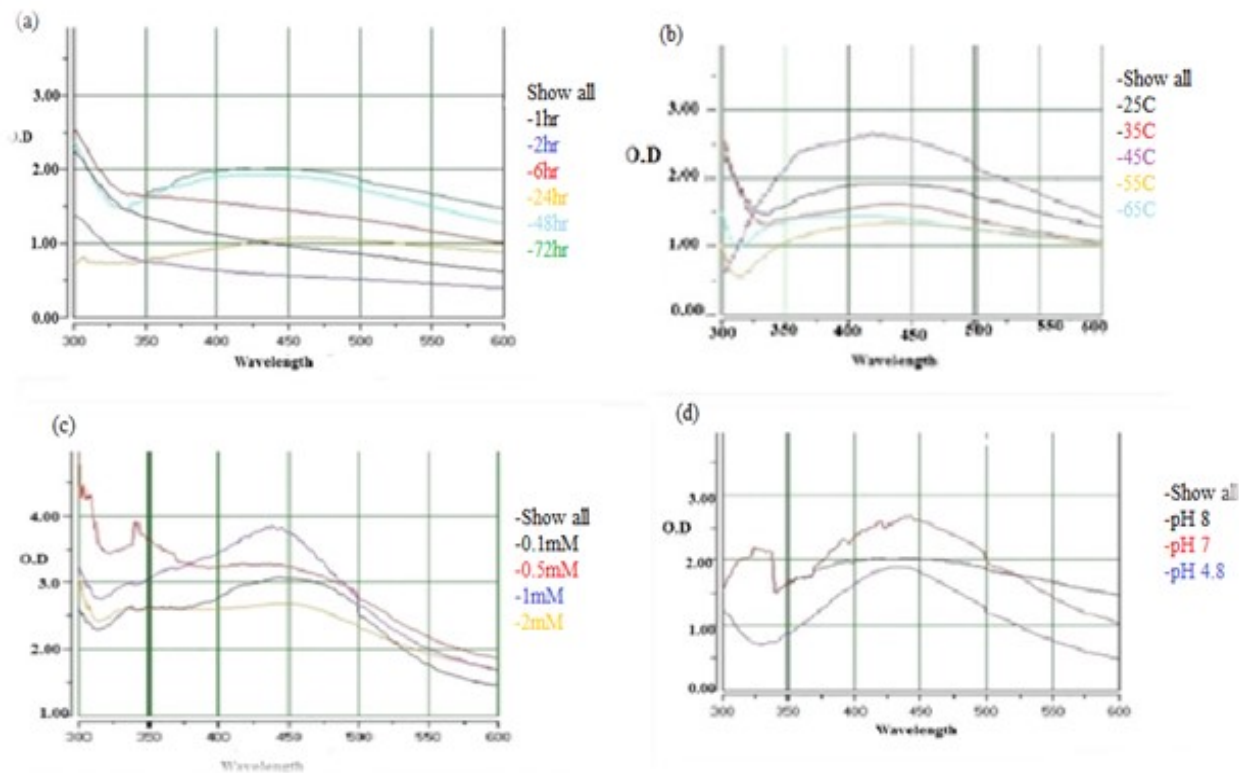


Fig. 2: Effect of incubation time, temperature, salt concentration and pH (a-d) on the synthesis of PAN

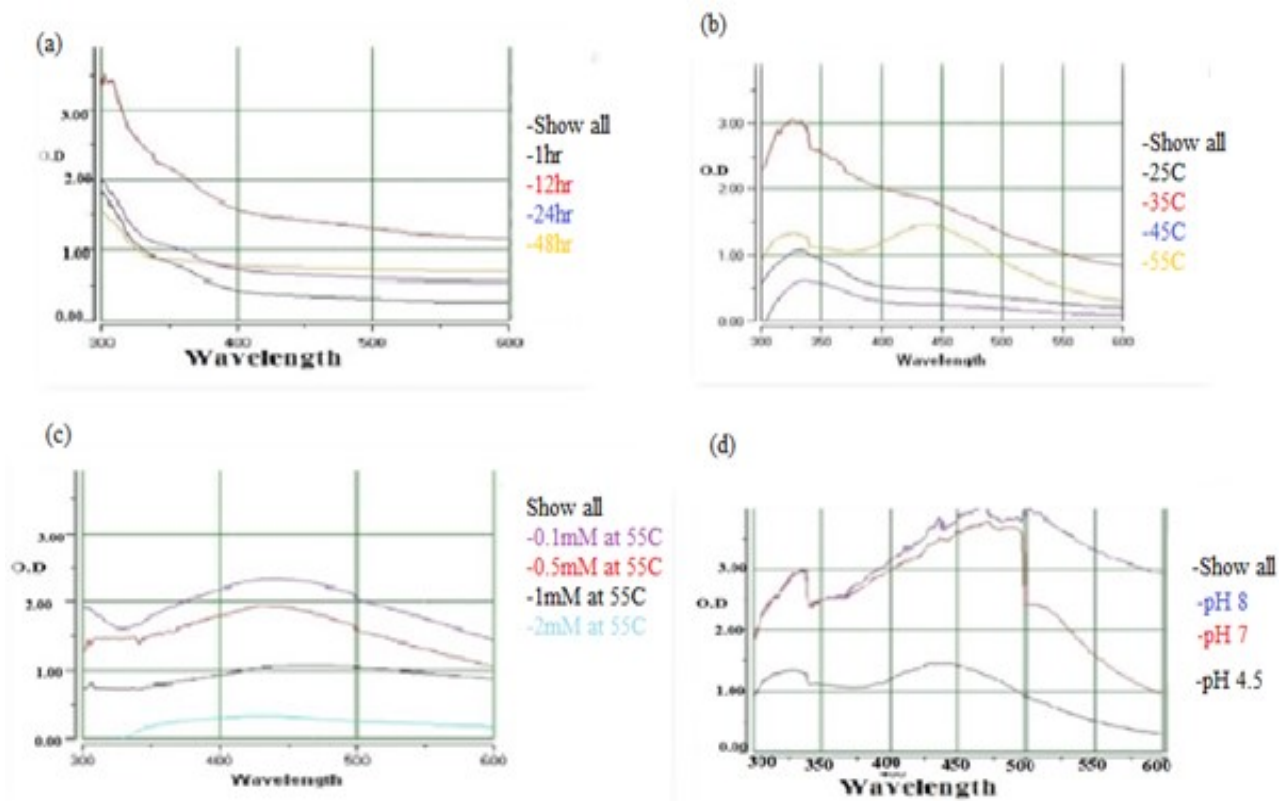
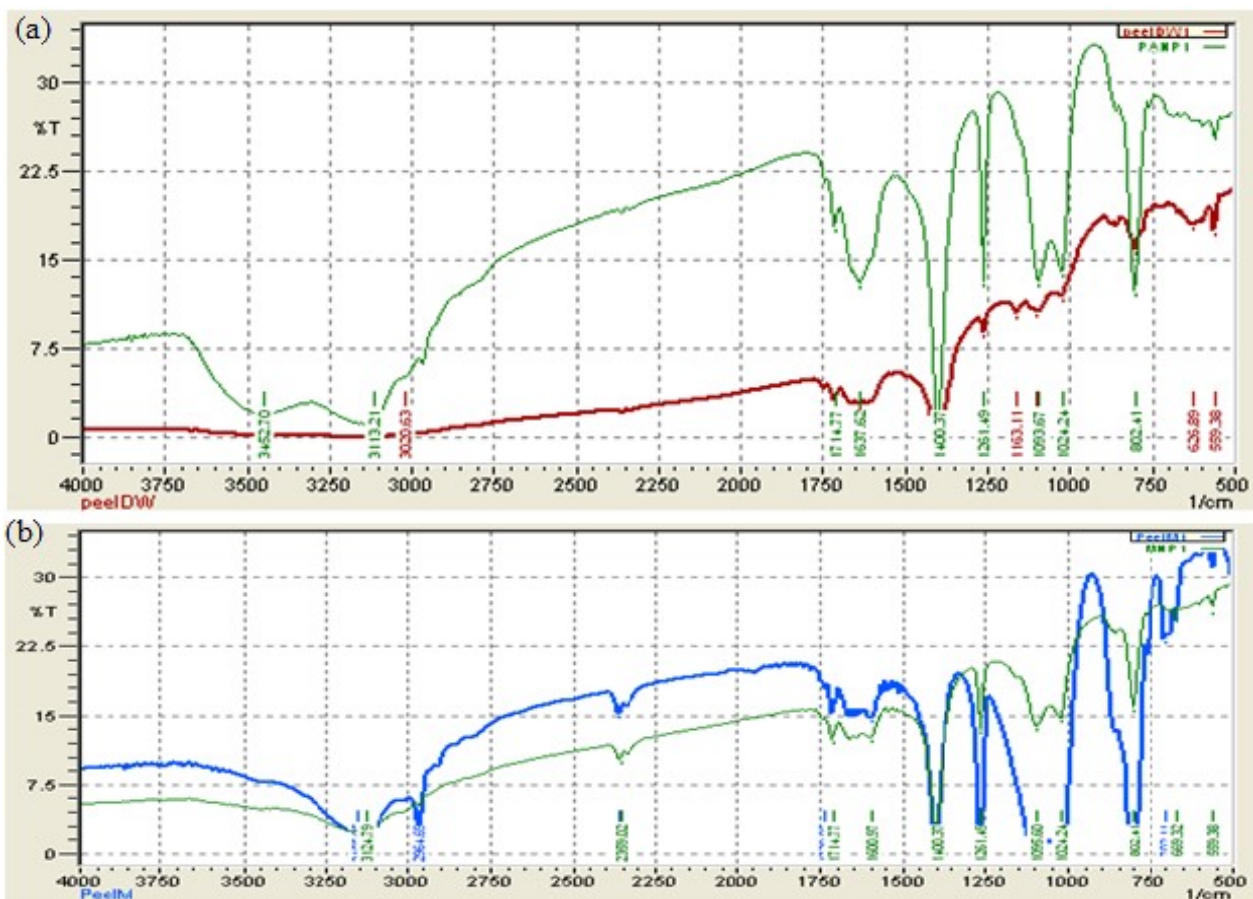
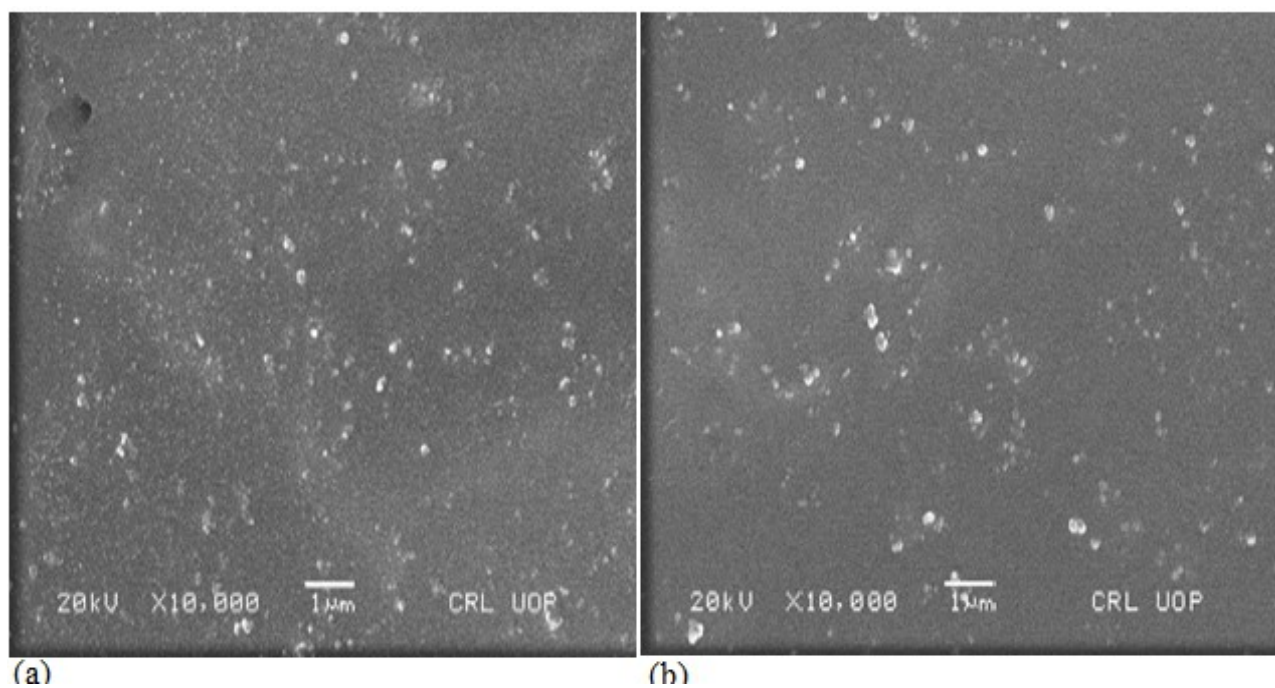


Fig. 3: Effect of incubation time, temperature, concentration of silver salt and pH (a-d) on the bio production of PMN



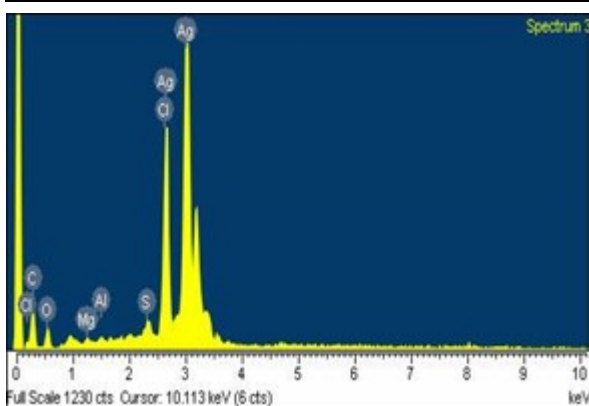
**Fig. 4:** FTIR for aqueous (a) methanolic (b) control of lychee peel in comparison to its synthesized nanoparticles. Red and blue peak shows the spectra of crude extract (control) whereas Green peaks refers to the spectra of silver nanoparticles



**Fig. 5:** Scanning electron microscopy of peel (a) PAN (b) PMN at resolution of 10,000X.

PMN the temperature clearly affected the process of silver reduction. U.V spectra shows peaks at wavelength region 445nm at 55°C, at 24 hours shown in fig. 3.

Element	Weight%	Atomic%
MgK	0.31	0.52
Ag L	57.00	17.02
CL	12.9	11.7
SK	0.9	0.92
CK	18.1	48.6
ALK	0.25	0.30
OK	10.34	20.8
Totals	100.00	



Element	Weight %	Atomic%
S	1.02	0.72
Ag L	44.44	9.38
ClK	3.6	2.3
OK	19.01	27.06
CK	31.2	60.1
Totals	100.00	

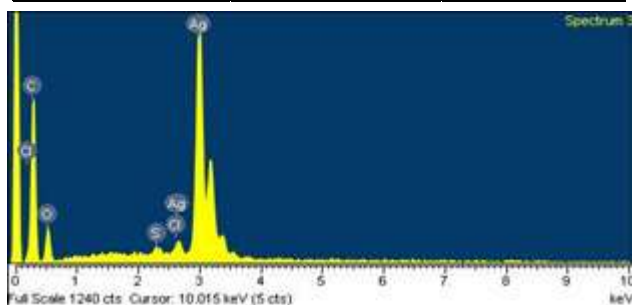


**Fig. 6:** Strong signal of silver (a) aqueous (b) methanolic byEnergy- dispersive spectrometer

Different concentration of silver nitrate PAN observed distant peak was at, 450nm wavelength o.1mM, at temperature of 35°C shown in fig. 2. A wider peak of PMN was obtained at 0.1mM ranges from 440-455 nm after 24 hours at 55°C temperature. The effect of different salt concentrations can be seen in fig. 3. After 48 hrs at 450nm as seen fig. 2, the best optimized pH for PAN is 4.8. After 24 hours, PMN displayed sharper peaks at pH 4.5 at 445nm, shown in fig 3. PMN a broader peak was obtained at 0.1mM ranges from 440-455nm at

temperature 55°C after 24 hours. fig. 3 shows the effect of different concentration of salts.

The best optimized pH for PAN is 4.8 after 48 hrs at 450nm absorbance shown in fig. 2. PMN showed distant peak at 445nm, pH 4.5 after 24 hours shown in fig 3.

pH 4.8, incubation time 48 hrs, 0.1mM salt concentration, temperature 35°C was the best optimized condition for the PAN. The PMN synthesized at 24 hours of the incubation time, with salt concentration of 0.1mM, 55°C temperature and pH 4.5.

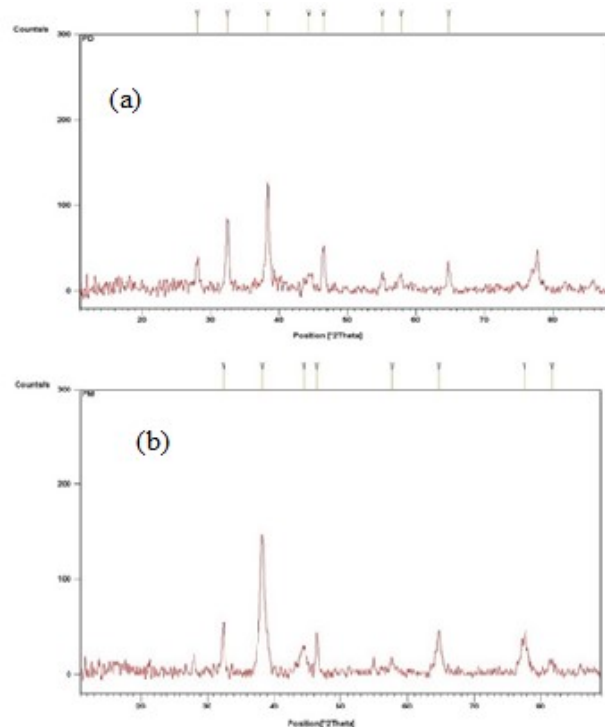


**Fig. 7:** Representative X-ray diffraction profile of (a) PAN (b) PMN

**Fourier Transform Infrared spectroscopy (FTIR)**

FTIR of peel control (aqueous) exhibited bands at 3020.63cm<sup>-1</sup>, 1714.77cm<sup>-1</sup>, assigned to NH<sub>3</sub> antisymmetrical stretch, H bonded OH. The absorption band at 1639.55cm<sup>-1</sup>, 1398.44cm<sup>-1</sup>, 1261.49cm<sup>-1</sup>, 1163.11cm<sup>-1</sup>, 1099.50cm<sup>-1</sup>, 1022.31cm<sup>-1</sup> and 800.49 cm<sup>-1</sup> corresponds to C=O stretch, CH out of plane deformations, C-N stretch. PAN showed IR peaks at 3452.70cm<sup>-1</sup>, 1714.77cm<sup>-1</sup>, 1637.62cm<sup>-1</sup>, 1400.37cm<sup>-1</sup>, 1261.49cm<sup>-1</sup>, 1093.67cm<sup>-1</sup>, 1024.24cm<sup>-1</sup> and 802.41cm<sup>-1</sup> due to possible groups like CN stretch, C-O-C stretch, NH stretch, C=O stretch. The peak at 3020.63 cm<sup>-1</sup>, 800.49cm<sup>-1</sup> in control (aqueous) were oxidized to 3452.70cm<sup>-1</sup> and 862.43cm<sup>-1</sup> containing NH stretch and OH hydroxyl group. Control (aqueous) sharp peak at 1163.11 cm<sup>-1</sup> was completely bio reduced during nanoparticles development due to SO<sub>2</sub>NH<sub>2</sub>. fig 4 display

the FTIR for (aqueous and methanolic) control with its biosynthesized nanoparticles.

Control (methanolic) extracts Fourier Transform Infrared spectroscopy absorbance bands were observed 3155.61 cm<sup>-1</sup>, 2964.65cm<sup>-1</sup>, 2360.73cm<sup>-1</sup>, assigned to NH stretch, NH<sub>3</sub> antisym stretch, C=O stretch. The various other bands 1739.85cm<sup>-1</sup>, 1600.97 cm<sup>-1</sup>, 1400.37 cm<sup>-1</sup>, 1261.51cm<sup>-1</sup>, 1095.60cm<sup>-1</sup>, 1024.24 cm<sup>-1</sup>, 802.41 cm<sup>-1</sup> represent CH out of plane deformation, C-O-C stretch, CN stretch, OH bending. FTIR of PMN showed bands at 3124.7cm<sup>-1</sup>, 2351.02cm<sup>-1</sup>, 1714.77cm<sup>-1</sup>, 1600.97cm<sup>-1</sup>, 1400.37cm<sup>-1</sup>, 1261.49cm<sup>-1</sup>, 1095.65cm<sup>-1</sup>, 1024.24cm<sup>-1</sup>, 802.41cm<sup>-1</sup> due to NH<sub>3</sub> antisym stretch, C=O stretch, CN stretch, PH stretch, NH<sub>2</sub> deformation, CH out of plane deformation. Peel control (methanolic) presented bio reduction of bands 3155.65cm<sup>-1</sup>, 702.77cm<sup>-1</sup> to 3124.79 cm<sup>-1</sup> and 669.32cm<sup>-1</sup>. Control (methanolic) band at 2964.69cm<sup>-1</sup> completely disappear in PMN confirming the presence of aliphatic compounds.

#### **Scanning electron microscopy with Energy Dispersive X-Rays analysis (SEM -EDX analysis).**

Scanning Electron Microscopy (SEM) showed PAN and PMN were mainly polycrystalline, less spherical and less homogenous in shape. Fig. 5 shows Scanning electron microscopy for PAN and PMN. The EDX profile showed strong signals for silver atom in PAN and PMN at 57.00 percent and 44.4 percent by weight percent respectively. Fig. 6 shows strong signals of elemental silver in the samples.

#### **X-Ray diffraction Study**

PAN was further demonstrated and confirmed by characteristics peaks observed in XRD image at  $\theta = 28.0646^\circ$ ,  $32.4925^\circ$ ,  $38.3533^\circ$ ,  $44.3065^\circ$ ,  $46.4932^\circ$ ,  $55.1106^\circ$ ,  $57.8029^\circ$ ,  $64.7559^\circ$  that indicated various planes as 100, 111, 200, 211, 220 of primitive cubic face centered. The average crystal particle size determined by using Debye Scherer's formula is taken as 6.9 nm. Fig. 7 shows Representative X-ray diffraction profile of PAN and PMN. The PMN showed peaks at  $32.4337^\circ$ ,  $38.3031^\circ$ ,  $44.430^\circ$ ,  $46.3808^\circ$ ,  $57.7012^\circ$ ,  $64.7344^\circ$ ,  $77.5280^\circ$ ,  $81.6178^\circ$  that index various planes as 110, 111, 220, 211, 311, 222 of the cubic face centered. The estimated average particle size for PMN is 7.9nm.

#### **Antibacterial activity of silver nanoparticles**

PAN showed highest antibacterial activity against *Alcaligenes faecium* (KJB33793)  $15\text{mm} \pm 0.005$  and  $20\text{mm} \pm 0.14$  at concentrations of 25 ug/ml and 50 ug/ml while least antibacterial activity showed by *Enterococcus faecium* (ORGIF) among all selected bacterial strain. PMN showed highest antimicrobial activity at concentrations of 25ug/ml and 50ug/ml against *Alcaligenes faecium* (KJB33793)  $15 \pm 0.153\text{mm}$  and  $17 \pm 0.1\text{mm}$ , *Mycobacterium oxidans* (KJ729148) showed inhibition

zones of  $15 \pm 0.064$  mm and  $17 \pm 0.05\text{mm}$ , *Bacillus subtilus* (KJ833777) against  $15 \pm 0.095$  and  $17 \pm 0.21\text{mm}$ . *Enterococcus faecium* (ORGIF) and *Klebsiella pneumoniae* (KJ833791) are two bacterial strains that showed the lower antibacterial activity against silver nanoparticles.

It is noted that *Klebsiella pneumoniae* (KJ833791) crude extracts and silver nitrate solution showed no antibacterial affect while PAN and PMN extracts showed inhibition zones as shown in Table 2. A two-way ANOVA test revealed a significant difference between bacterial strains in PAN and PMN samples at different concentrations tested for antibacterial activity (Supplementary Table).

#### **Minimum Inhibitory Concentrations (MIC)**

A systematic study was done to determine Minimum Inhibitory Concentrations (MIC) of silver nanoparticles against various bacterial strains. The MIC values for PAN and PMN were detected in the range of 15-25 $\mu\text{g/ml}$ . PAN MIC values was measured against the bacterial strains *Mycobacterium oxidans* (KJ729148), *Alcaligenes faecium* (KJB33793), *Bacillus subtilus* (KJ833777) was 20ug/ml. For PMN minimum inhibitory (MIC) concentration of *Alcaligenes faecium*(KJB33793) and *Mycobacterium oxidans*(KJ729148) is 15ug/ml, followed by a strain of *Bacillus subtilus*(KJ833777) of 20ug/ml. PAN and PMN MIC values for *Klebsiella pneumonia* (KJ833791), *Pseudomonas geniculate* (KJ729146), *Streptomyces laurentii* (KJ729145) and *Enterococcus faecium*(ORGIF) are 25ug/ml.

## **DISCUSSION**

*Litchi chinensis* was chosen for green silver nanoparticles biosynthesis. Comparative research was carried out to find the different parameters like temperature, effect of salt concentration, pH, and time of incubation on silver ion reduction. *Litchi chinensis* qualitative and quantitative screening indicated that peel (aqueous and methanolic extracts) is richer in bioactive constituents as compared to seed (aqueous and methanolic) extracts. Alkaloids, flavonoids, saponins and other phytochemical constituents are involved in various applications like antibacterial activity, antifungal, anti-cancerous, antimalarial and insecticidal (Hamidpour *et al.*, 2015; Dong *et al.*, 2019).

The most possible mechanisms of nanostructured silver ions are attributable to the capacity to donate electrons found in peel extract. Due to electron donation potential of alkaloids, the alkaloid content in *Litchi chinensis* peel extracts promotes the bio reducing silver metal ions to nanoscale silver. Flavonoids are capable of binding flavanones to nanoparticles surface. In flavonoids, ketone group is converted into carboxylic acid to demonstrate bio reduction of silver metal ions. Phenolic are powerful antioxidants that cause silver ions to reduce to the nanosized silver stated in (Dubey *et al.*, 2010). Silver ions

may form multiplexes with phenolic hydroxyl OH groups which subsequently oxidize the form of quinone resulting in silver (Ag<sup>+</sup>) reduction to nanoparticles. The quinoid formed by phenol group oxidation and adsorbed on the nanoparticles stabilized surface.

Different parameters are selected for optimization of nanoparticles synthesis. Biogenic nanoparticles production started within 45 minutes due to the particles' growth in size. Once the incubation time was raised, the colour change is increased. The colour displayed by metallic nanoparticles is due to the oscillation within the band gap of "free" electrons, which leads to an excitation in process, defined as surface plasmon resonance. There is a dark blackish brown colour of nanoparticles that accumulated at the conical flask base.

PAN showed most prominent (SPR) band at 428 and 450 nm wavelength recorded at temperature of 35°C and 45°C. Prominent peaks indicated that at temperature 35°C and 45°C the silver nanoparticles production increases due to upsurge in nucleation reaction.

PMN required higher temperature 55°C with an incubation time of 24 hours for nanoparticles synthesis. By changing pH of the reaction mixtures, biogenic nanoparticles synthesis can be operated. By modifying pH, the electrical charges of green compounds disturbing the capping and stabilizing abilities and nanoparticles production (Javed *et al.*, 2020). Silver salt concentration with plant extract (1:1 ratio) gives rise to the growth of nanoparticles such as Ostwald ripening. This provides surface plasmon resonance (SPR) band a red change (on the way to a lengthier wavelength) due to nanoparticles stabilization by the biomolecules of plants that act as functional stabilizing agent.

FTIR is used for identification of various functional groups in fruit extracts. FTIR bands such as, from aliphatic chains (NH stretching hydrogen bond), CH stretching of the CH<sub>2</sub> groups, specifies amino acids group presence and C=O (from aromatic rings) stretching vibrations. The majority of IR bands are the characteristics of different functional groups as phenols, proteins, alkaloids, saponins, flavonoids, tannins, phenols, glycosides, polyphenol groups and secondary amides and alcohols (Oliveira *et al.*, 2016; Garibo *et al.*, 2020).

Scanning electron microscopy of prepared PAN and PMN revealed to be polycrystalline and less homogenous. Spherical shaped silver nanoparticles from green extracts have also been reported by many research groups (Rautela *et al.*, 2019).

X-Ray Diffraction (XRD) pattern shows prepared PAN and PMN of an average size of 6.9nm and 7.9nm of primitive cubic phases. The cubic phase of silver

nanoparticles are observed in *Solanum xanthocarpum* contains silver nanoparticles of size 4-18nm (Gardea-Torresdey *et al.*, 2003)

This research contains green synthesis of silver nanoparticles and their bactericidal action were study against selected gram positive and gram negative bacterial strains. *Bacillus subtilius*, *Enterococcus faecium* and *Streptomyces laurentii* is a Gram-positive bacteria. *Pseudomonas geniculate*, *Mycobacterium oxidans*, *Alcaligenes faecium* and *Klebsiella pneumoniae* a Gram-negative shaped bacterium. The highest bactericidal activity of PAN and PMN was found effective against *Alcaligenes faecium*. Crude extract and AgNO<sub>3</sub> salt solution did not showed no bactericidal activity against *Klebsiella pneumoniae*. Interestingly, silver nanoparticles were tested against *Klebsiella pneumoniae* that showed inhibition zones. The silver salt and peel extract mixture has shown a 2-fold increase in bactericidal values for this cause.

Minimum inhibitory concentration (MIC) zones distinction between the diverse bacteria is due to complex bacterial structure such as peptidoglycan and mostly comprehends negatively charged lipoteichoic acid or teichoic acid. The restoration of free positive charged Ag<sup>+</sup> ions can be facilitated by this negative charge on bacteria. Gram-positive bacteria can allow silver to enter into the cytoplasmic membrane and have shown better bactericidal activity compared to gram-negative bacteria.

Several mechanisms for antibacterial activities provided by silver nanoparticles have been introduced. One school of thought suggests that silver nanoparticles enter deeply into the bacterial membrane or respiratory chain, and that their cell cycle contributes to bacterial cell death (Ahmad *et al.*, 2016). The nanostructures within regulate the signal transduction of protein substrates in bacteria due to phosphorylation phenomena. The silver ions are the reserves of enzymes comprising the thiol group, e.g. in the respiratory system, NADH-dehydrogenase II is involved. The NADH dehydrogenase II reticence contributes to boost in free radical production. The cells then need hydrogen peroxide concentration that is free from radicals to be reduced. ROS can induce bacterial cell apoptosis that eventually, lead to death.

## CONCLUSION

The feasibility of using aqueous peel and methanolic extracts of *Litchi chinensis* for the biogenic, green and eco-friendly biosynthesis of AgNPs was demonstrated in this research. With sizes ranging from 6.9 nm, PAN is circular, primitive cubic face based and PMN was 7.9 nm. The particles showed strength against clinical bacterial isolates that are multidrug-resistant, thereby establishing the significance of biosynthesized silver nanoparticles in

biomedical applications. Therefore, it can be inferred that *Litchi chinensis* extracts find useful applications in the biosynthesis of novel nanoparticles, thus growing the plant's biotechnological potential.

## REFERENCES

- Ahmad A, Wei Y, Syed F, Tahir K and Ur A (2016). The effects of bacteria-nanoparticles interface on the antibacterial activity of green synthesized silver nanoparticles microbial pathogenesis the effects of bacteria-nanoparticles interface on the antibacterial activity of green synthesized silver nanopa. *Microb. Pathog.*, **102**(10): 133-142.
- Coker GH, Adesegun S, Adepoju-Bello A, Obaweya K, Ezennia E and Atangbayila T (2008). Phytochemical screening and antioxidant activities of some selected medicinal plants used for malaria therapy in southwestern Nigeria. *Trop. J. Pharm. Res.*, **7**(3): 1019-1024.
- Chenthamara D, Subramaniam S, Ramakrishnan SG, Krishnaswamy S, Essa MM, Lin FH and Qoronfleh MW (2019). Therapeutic efficacy of nanoparticles and routes of administration. *Biomater. Res.*, **23**(20): 1-29.
- Dong X, Huang Y, Wang Y and He X (2019). Anti-inflammatory and antioxidant jasmonates and flavonoids from lychee seeds. *J. Funct. Foods*, **54**(10): 74-80.
- Dubey SP, Lahtinen M, Särkka H and Sillanpää M (2010). Bioprospective of *Sorbus aucuparia* leaf extract in development of silver and gold nanocolloids. *Colloids Surfaces B Biointerfaces*, **80**(1): 26-33.
- Emanuele S, Lauricella M, Calvaruso G, D'Anneo A, Giuliano M (2017). *Litchi chinensis* as a functional food and a source of antitumor compounds: An overview and a description of biochemical pathways. *Nutrients*, **8**(9): 992.
- Gardea-Torresdey JL, Gomez E, Peralta-Videa JR, Parsons JG, Troiani H and Jose-Yacamán M (2003). Alfalfa sprouts: A natural source for the synthesis of silver nanoparticles. *Langmuir*, **19**(4): 1357-1361.
- Garibo D, Nunez HAB, Leon JND De, Mendoza EG, Estrada I, Magaña YT, Tiznado H, Marroquin MO, Ramos AGS, Blanco A, Rodríguez JA, Romo OA, Almazán LAC and Arce AS (2020). Green synthesis of silver nanoparticles using *Lysiloma acapulcensis* exhibit high-antimicrobial activity. *Sci. Rep.*, **10**: Article number: 12805.
- Hamidpour M, Hamidpour S and Shahlari M (2015). Cinnamon from the selection of traditional applications to its novel effects on the inhibition of angiogenesis in cancer cells and prevention of Alzheimer's disease, and a series of functions such as antioxidant, anticholesterol, antidiabetes, antibacterial, antifungal, nematocidal, acaracidal, and repellent activities. *J. Tradit. Complement. Med.*, **5**(2): 66-70.
- Iqbal E, Salim KA and Lim LBL (2015). Phytochemical screening, total phenolics and antioxidant activities of bark and leaf extracts of *Goniothalamus velutinus* (Airy Shaw) from Brunei Darussalam. *J. King Saud Univ. Sci.*, **27**(3): 224-232.
- Javed R, Zia M, Naz S, Aisida SO, Ain N ul and Ao Q (2020). Role of capping agents in the application of nanoparticles in biomedicine and environmental remediation: recent trends and future prospects. *J. Nanobiotechnology*, **18**(172): 1-15.
- Khan T, Ali M, Khan A, Nisar P, Jan SA, Afridi S and Shinwari ZK (2020). Anticancer plants: A review of the active phytochemicals, applications in animal models, and regulatory aspects. *Biomolecules* **10**(1): 47.
- Kifle ZD, Yesuf JS and Atnafie SA (2020). Evaluation of in vitro and in vivo anti-diabetic, anti-hyperlipidemic and anti-oxidant activity of flower crude extract and solvent fractions of *Hagenia abyssinica* (Rosaceae). *J. Exp. Pharmacol.*, **12**(1): 151-167.
- Mogana R, Adhikari A, Tzar MN, Ramliza R and Wiart C (2020). Antibacterial activities of the extracts, fractions and isolated compounds from *Canarium patentinervium* Miq. against bacterial clinical isolates **5**(1): 1-11.
- Mukundi MJ (2015). Antidiabetic effects of aqueous leaf extracts of *Acacia nilotica* in alloxan induced diabetic mice. *J. Diabetes Metab.*, **6**(7) DOI: 10.4172/2155-6156.1000568
- Njagi EN, Mwaniki MJM, Njagi J and Murugi NMP (2015). In vivo anti-diabetic effects of aqueous leaf extracts of *Rhoicissus tridentata* in alloxan induced diabetic mice. *J. Dev. Drugs*, **4**: 3-9.
- Oliveira RN, Mancini MC, De Oliveira FCS, Passos TM, Quilty B, Thire RM, da SM and McGuinness GB (2016). Análise por FTIR e quantificação de fenóis e flavonóides de cinco produtos naturais disponíveis comercialmente utilizados no tratamento de feridas. *Rev. Mater.*, **21**: 767-779.
- Pirtarighat S, Ghannadnia M, Baghshahi S (2019). Green synthesis of silver nanoparticles using the plant extract of *Salvia spinosa* grown in vitro and their antibacterial activity assessment. *J. Nanostructure Chem.*, **9**: 1-9.
- Rautela A, Rani J, Das MD (2019). Green synthesis of silver nanoparticles from *Tectona grandis* seeds extract: Characterization and mechanism of antimicrobial action on different microorganisms. *J. Anal. Sci. Technol.*, **10**: 5.
- Rose GK, Soni R, Rishi P, Soni SK (2019). Optimization of the biological synthesis of silver nanoparticles using *Penicillium oxalicum* GRS-1 and their antimicrobial effects against common food-borne pathogens. *Green Process. Synth.* **8**(1): 144-156.
- Salehi B, Ata A, Kumar NVA, Sharopov F, Ramírez-Alarcon K, Ruiz-Ortega A, Ayatollahi SA, Fokou PVT, Kobarfard F, Zakaria ZA, Iriti M, Taheri Y, Martorell M, Sureda A, Setzer WN, Durazzo A, Lucarini M, Santini A, Capasso R, Ostrander EA, Atta-ur-Rahman, Choudhary MI, Cho WC and Sharifi-Rad J (2019).

Antidiabetic potential of medicinal plants and their active components, *Biomolecules*. **9**(10): 551.  
 Zhao L, Wang Kun, Wang Kai, Zhu J and Hu Z (2020). Nutrient components, health benefits and safety of

litchi (*Litchi chinensis* Sonn.): A review. *Compr. Rev. Food Sci. Food Saf.*, **19**(4): 2139-2163.

### Supplementary Materials

**Table 1:** Two -way ANOVA parameters for statistical variance in different bacterial strains towards PAN at concentration of 25 and 50ug/ml

ANOVA						
Source of Variation	SS	df	MS	F	P-value	F crit
Bacterial Strains	86.71429	6	14.45238	19.58065	0.001065	4.283866
Concentrations	28.57143	1	28.57143	38.70968	0.000797	5.987378
Error	4.428571	6	0.738095			
Total	119.7143	13				

**Table 2:** Two -way ANOVA parameters for statistical variance in different bacterial strains towards PMN PMA at concentration of 25 and 50ug/ml

ANOVA						
Source of Variation	SS	df	MS	F	P-value	F crit
Bacterial Strains	92.66857	6	15.44476	43.01592	0.000113	4.283866
Concentrations	15.22571	1	15.22571	42.40584	0.000625	5.987378
Error	2.154286	6	0.359048			
Total	110.0486	13				

**Table 3:** Two -way ANOVA parameters for statistical variance in different bacterial strains towards Control and PAN (50ug/ml)

ANOVA						
Source of Variation	SS	df	MS	F	P-value	F crit
Bacterial Strains	340.35	5	68.07	1.233376	0.411786	5.050329
Control and PAN	104.43	1	104.43	1.892191	0.227383	6.607891
Error	275.95	5	55.19			
Total	720.73	11				

**Table 4:** Two -way ANOVA parameters for statistical variance in various bacterial strains towards Control and PMN (50ug/ml)

ANOVA						
Source of Variation	SS	df	MS	F	P-value	F crit
Bacterial Strains	344.7767	5	68.95533	1.282381	0.395783	5.050329
Controls and PMN	106.8033	1	106.8033	1.98625	0.217789	6.607891
Error	268.8567	5	53.77133			
Total	720.4367	11				